

An Alternative View of Filter-Cake Formation in Fractures Inspired by Cr(III)-Acetate-HPAM Gel Extrusion

R.S. Seright, SPE, New Mexico Petroleum Recovery Research Center

Summary

A new model was developed to describe water leakoff from formed Cr(III)-acetate-HPAM gels during extrusion through fractures. This model is fundamentally different from the conventional filter-cake model used during hydraulic fracturing. Even so, it accurately predicted leakoff during extrusion of a guar-borate gel. Thus, the new model may be of interest in hydraulic fracturing. Contrary to the conventional one, the new model correctly predicted the occurrence of wormholes and stable pressure gradients during gel extrusion through fractures.

Introduction

This work was motivated by an attempt to understand the propagation of formed gels as they extrude through fractures during water shutoff treatments. Earlier works¹⁻⁶ revealed that formed gels lost water during extrusion through fractures and that water leakoff controlled the rate of gel propagation. Leakoff was also known to control the rate of fracture growth during hydraulic fracturing⁷⁻¹¹ and during produced water reinjection.¹²⁻¹⁴

In the conventional view of hydraulic fracturing, the leakoff rate was determined by one (or a combination) of three mechanisms.^{7,8,10}

- Propagation of the fracturing fluid front into the rock matrix (i.e., away from the fracture face).
- Reservoir fluid viscosity/compressibility effects.
- The formation of a filter cake associated with particulate matter that was suspended in the fracturing fluid.

The latter mechanism may involve formation of a filter cake on the fracture surface (i.e., an external filter cake) and/or penetration of the particulates some distance into the porous rock (i.e., an internal filter cake). This paper focuses on leakoff that is dominated by the formation of an external filter cake in a fracture, first reviewing the conventional filter-cake model and then presenting experimental evidence that questions a key assumption of the conventional model. Next, an alternative model is presented, and then important differences in predictions from both are discussed. This paper also examines gel behavior in fractures as a function of temperature, composition, and brine injection after placement.

Conventional Filter-Cake Model

The widely accepted model of filter-cake formation was introduced by Carter.^{7,8,10} Assume that a particulate-laden fluid contacts a rock interface (i.e., a fracture face) and a pressure difference, Δp , exists between the fracture and the porous rock. As solvent (with viscosity μ) flows into the rock at a velocity u_f , the particulates form a filter cake of permeability k and thickness L . At any given time, the filtrate velocity (i.e., the leakoff rate) is given by the Darcy equation.

$$u_f = k \Delta p / (\mu L) \dots \dots \dots (1)$$

The thickness of an incompressible filter cake grows at a rate that is proportional to filtrate throughput.

$$L = \int u_f dt / \alpha, \dots \dots \dots (2)$$

in which α = the factor by which the particulates are concentrated during the transition from suspension to the filter cake. Combining Eqs. 1 and 2 yields Eq. 3.

$$u_f = \alpha k \Delta p / (\mu \int u_f dt) \dots \dots \dots (3)$$

Eq. 4 presents a solution to Eq. 3.

$$u_f = [\alpha k \Delta p / (2\mu)]^{0.5} (t - t_{exp})^{-0.5}, \dots \dots \dots (4)$$

in which t_{exp} = the time of first exposure to filter cake for the element of fracture face of interest. The key result in Eq. 4 is that the leakoff rate is proportional to $t^{-0.5}$. This proportionality was often verified experimentally, especially during static filtration experiments.^{7,9,10} An important assumption in the development of Eq. 4 was that the filter-cake thickness was uniform at any given time. The next two sections will present evidence that questions this assumption.

Gel Behavior in Fractures

Before gelation, fluid gelant solutions can readily leak off from fractures into porous rock.¹⁵ After gelation, however, the crosslinked materials will not penetrate significantly into the porous rock.¹⁻⁶ Thus, formed gels must extrude through fractures during the placement process. In other words, the crosslinked polymer moves through the fracture as a semisolid and does not penetrate past the fracture faces into the porous rock.

The pressure gradients required to extrude gels through fractures are greater than those for gelant flow. Depending upon conditions, the effective viscosity of formed gels in fractures is typically between 10^3 and 10^6 times greater than those for gelants.¹ However, useful gels do not show progressive plugging during extrusion through fractures. This point is illustrated in Fig. 1, in which 75 fracture volumes (3500 cm^3 or 213 in.^3) of Cr(III)-acetate-HPAM gel were extruded through a fracture (in a $48 \times 1.5 \times 1.5$ -in. Berea core) at a fixed rate of $2000 \text{ cm}^3/\text{hr}$ ($4,130 \text{ ft/D}$). After gel breakthrough at the end of the 4-ft-long fracture, the pressure gradient was stable at 13.5 psi/ft. In other experiments with this gel, the pressure gradients sometimes showed greater variations than those illustrated in Fig. 1.² These variations may result from temporary gel screenouts that form and break during the extrusion process. However, in general, the pressure gradients do not steadily increase with increased time and gel throughput. This behavior is necessary to propagate formed gels deep into a fracture or fracture system. Of course, the presence or absence of this desirable behavior depends on the gel and the extrusion conditions. Some gels show dramatic screenouts and progressive plugging.³

For Cr(III)-acetate-HPAM gels, a minimum pressure gradient was required to extrude the gel through a fracture with a given width.¹ Once the minimum pressure gradient was exceeded, the pressure gradient during gel extrusion was insensitive to the flow rate. For example, in a 0.04-in.-wide fracture,⁴ a 1-day-old gel with 0.5% HPAM and 0.0417% Cr(III)-acetate exhibited a pressure gradient that averaged 28 psi/ft for injection fluxes between 413 and 33,100 ft/D. The gel mechanical degradation was fairly small. For gel produced from the fracture at the highest rate, the elastic modulus was approximately 20% less than that of the original. In all cases, the physical appearance of the gel remained unchanged by passage through the fracture.

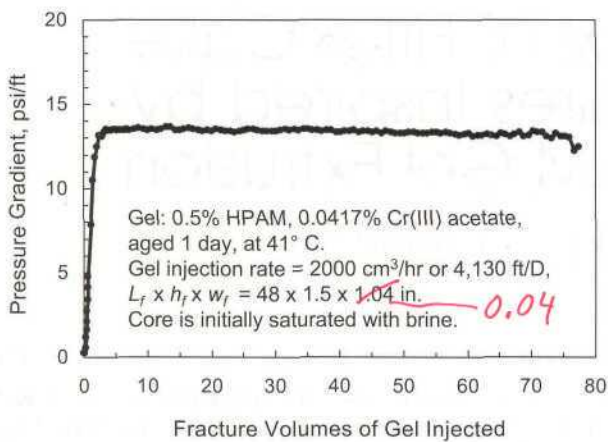


Fig. 1—Pressure gradients in a fracture during gel extrusion.

For fractures with widths between 0.006 and 0.4 in., the pressure gradient required for gel extrusion varied inversely with the square of the fracture width (see Fig. 2).^{1,2,16} This behavior was directly tied to the pressure gradient's insensitivity to changes in the flow rate. Ref. 5 demonstrated mathematically that if the pressure gradient is independent of the flow rate (for a fracture with a given width), then it should vary inversely with the square of the fracture width.

Cr(III)-acetate-HPAM gels (as well as other gels) concentrate or lose water during extrusion through fractures, reducing the rate of gel propagation.¹⁻⁶ When large volumes of gel were extruded through a fracture, the effluent had the same appearance and a similar composition as those for the injected gel, even though a concentrated, immobile gel formed in the fracture. During gel extrusion, water leaked off, and the gel concentrated to become immobile in the vicinity of where dehydration occurred. Crosslinked polymer did not penetrate significantly into the porous rock. The driving force for gel dehydration (and water leakoff) was the pressure difference between the fracture and the adjacent porous rock. Fresh gel (i.e., mobile gel with the original composition) wormholed through the concentrated one to advance the gel front (see Fig. 3). At a given position along the fracture, the average gel concentration increased, and the fracture area contacted by wormholes (i.e., mobile gel) decreased with time.^{2,5} Even so, water

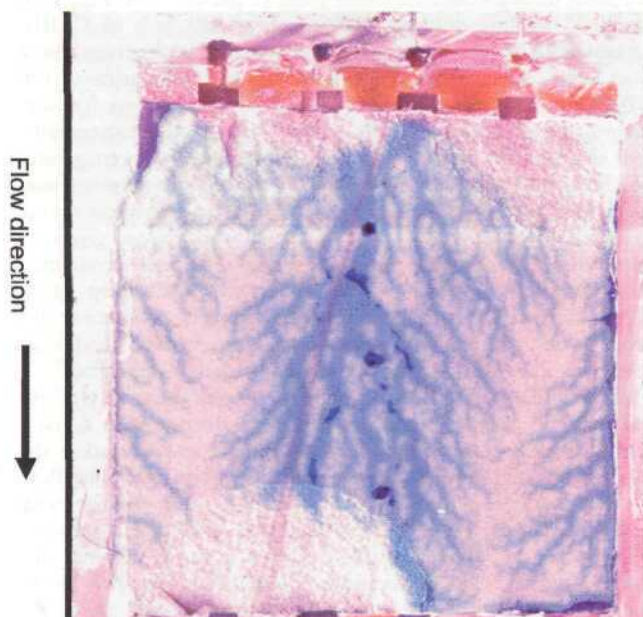


Fig. 3—Wormhole pattern during dyed gel injection following gel of the same composition (not dyed).

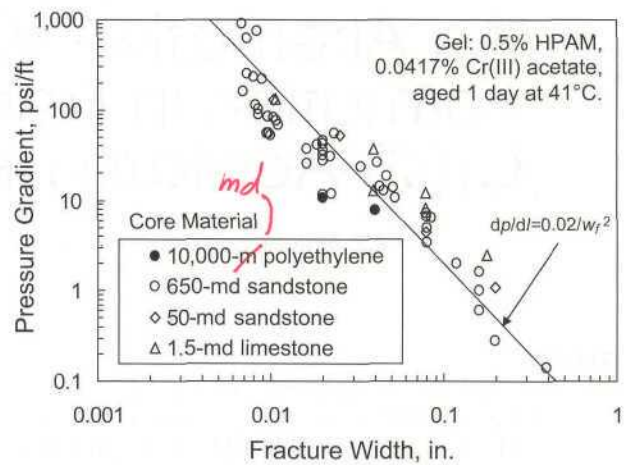


Fig. 2—Pressure gradients required to extrude gels through fractures.

leakoff from the concentrated, immobile gel was generally small compared with leakoff from the mobile gel.^{5,16,17} During gel extrusion through a fracture of a given width, the pressure gradients along the fracture and the dehydration factors were the same for fractures in 650-md sandstone as in 50-md sandstone, 1.5-md limestone, and 10,000-md polyethylene cores (see Fig. 2).^{1-6,16}

For a Cr(III)-acetate-HPAM gel, dehydration was quantified for a significant range of conditions.¹⁻⁶ For fracture widths from 0.02 to 0.16 in., lengths from 0.5 to 32 ft, heights from 1.5 to 12 in., and injection fluxes from 129 to 66,200 ft/D, the average rate of gel dehydration and leakoff (u_l , in ft/D or ft³/ft²/D) was described reasonably well with Eq. 5,

$$u_l = 0.05t^{-0.55} \quad (5)$$

in which t = time in days. Fig. 4 summarizes the leakoff results.⁶

On first consideration, Eq. 5 and the dashed line in Fig. 4 appeared to support the conventional view of filter-cake formation in hydraulic fractures (i.e., because leakoff varied with $t^{-0.5}$ as suggested by Eq. 4). However, the conventional model assumed that a uniform filter cake formed. In contrast, our experiments revealed that fresh gel wormholed through concentrated gel, resulting in a distinctly nonuniform distribution of the filter cake on the fracture faces. Fig. 3 shows the wormhole pattern that developed during one experiment.⁵ (The dimensions of the fracture shown in Fig. 3 were $L_f \times h_f \times w_f = 12 \times 12 \times 0.04$ in.) Early in the gel-injection process, the wormhole pattern was very branched,

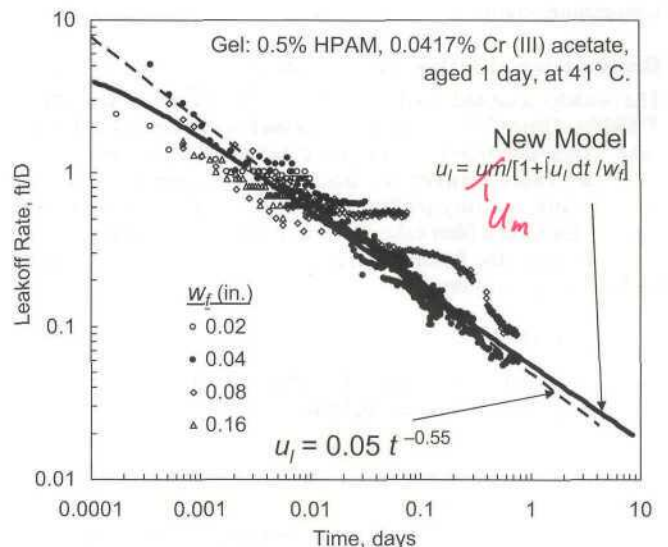


Fig. 4—Summary of leakoff data at 41° C.

with a significant fraction of the fracture area contacted (as in Fig. 3).⁵ As additional gel volumes were injected, the wormholes became less branched and a diminished fraction of the fracture area was contacted by the wormholes.⁵ This behavior was not surprising because the dehydrated gel became increasingly concentrated and less mobile, and the mobility ratio (mobility of fresh gel divided by mobility of concentrated gel) increased with gel throughput.

A second failure of the conventional filter-cake model occurs with its prediction of pressure behavior vs. gel throughput. In particular, the model predicts that the filter cake on the fracture walls should uniformly increase in thickness with time, thereby decreasing the width of the active flow path in the fracture (see the left side of Fig. 5, which greatly exaggerates fracture width relative to fracture height). Because the pressure gradient required for gel extrusion increases significantly with decreasing channel width (Fig. 2), the conventional model predicts that these should increase substantially with increased time and gel throughput. Fig. 1 demonstrates that this prediction is incorrect; after gel breakthrough, pressure gradients are reasonably stable during gel extrusion.

New Mechanistic Model for Leakoff

The previous observations inspired a new mechanistic model of gel propagation and dehydration in fractures. Consistent with our experimental results, this model assumed the following.

1. Water can leave the gel and leak off through the fracture faces, but crosslinked polymer cannot.
2. Mobile gel has the same composition as injected gel.
3. When an element of mobile gel dehydrates, that gel becomes immobile. For a given vicinity and time, t , in a fracture of width, w_f , the average gel concentration (C/C_o , which gives the gel concentration, C , relative to the concentration for the injected gel, C_o) is

$$C/C_o = 1 + \int u_l dt / w_f \dots \dots \dots (6)$$

in which u_l = the average leakoff rate for that vicinity. The process of transforming an element of mobile gel into concentrated, immobile gel may occur very rapidly. However, for the purposes of our model, this transition does not need to occur in zero time.

4. At a given point along the fracture, the fracture surface is covered by either mobile (with fractional area, A_m) or immobile gel (with fractional area, A_c) so that

$$A_m + A_c = 1 \dots \dots \dots (7)$$

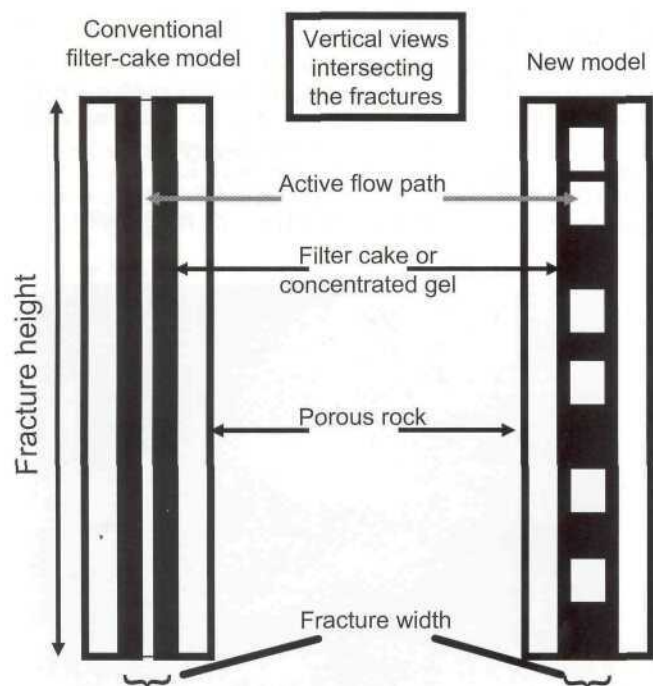


Fig. 5—Illustration of the conventional filtration model vs. the new one.

The fraction of surface that contacts mobile gel decreases with time as more immobile gel forms. Based on area and mass balances, the fractional area covered by concentrated gel at a given time and vicinity is approximated by

$$A_c = [C/C_o - 1] / [C/C_o] \dots \dots \dots (8)$$

Presumably, as mobile gel in a wormhole dehydrates, a thin layer of concentrated gel forms at the fracture surface. However, this thin layer is continually pushed aside by leakoff water or mobile gel, and concentrated gel is added to the accumulation of immobile gel at the sides of the wormhole. In Ref. 16, our model is shown to work reasonably well when the right side of Eq. 8 is taken to any power between 0.25 and 4.

5. Water leakoff from immobile (dehydrated) gel (u_c) is negligible compared to that from the mobile gel (u_m). (The immobile gel continues to concentrate and lose water with time. However, this leakoff rate is small compared to that from the much more permeable mobile gel. The validity of this assumption was demonstrated in Refs. 5, 16, and 17.)

$$u_m \gg u_c \dots \dots \dots (9)$$

6. The mobile gel has a finite permeability to water (k_{gel}) that provides a fixed local leakoff flux (u_m) for the fracture surface that is in direct contact with the mobile gel (i.e., the wormhole area in contact with the fracture faces).

$$u_l \approx A_m u_m \dots \dots \dots (10)$$

Combining Eqs. 6 through 10 yields Eq. 11, which is the basis of the new model. The model predicts the leakoff rate (i.e., the rate of gel dehydration) at a given time and distance along the gel-contacted portion of a fracture.

$$u_l = u_m / [1 + \int u_l dt / w_f] \dots \dots \dots (11)$$

The denominator of Eq. 11 reflects the loss rate for the fracture surface where it is contacted by mobile gel (i.e., the wormhole-contact area). For our 1-day-old Cr(III)-acetate-HPAM gel, u_m has a value of approximately 4 ft/D, which translates to a k_{gel} value of approximately 1 md. The latter value was confirmed from independent experiments.¹⁷ The fraction of the fracture area contacted by concentrated gel is plotted vs. time in Fig. 6. This plot indicates that after 0.0007 days (1 minute) of gel contact, at least 50% of the fracture face is covered by concentrated rather than fresh gel. Within 0.02 days (30 minutes) of gel contact, more than 90% of the fracture face is covered by concentrated gel.

At a given distance along a fracture, the new model predicts that the wormhole area diminishes and that the wormholes become more widely spaced with time. Consequently, one might expect pressure gradients to develop within the fracture transverse to the direction of flow. However, the compliant nature of the gel (even

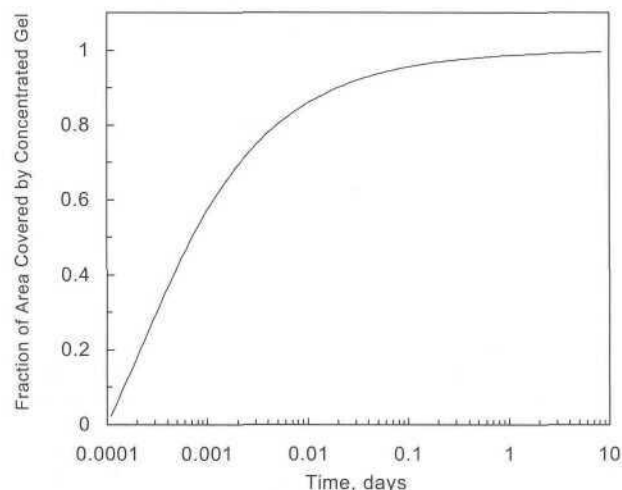


Fig. 6—Fraction predictions for fracture area contacted by concentrated gel.

concentrated gel) mitigates the development of these transverse pressure gradients.

Leakoff predictions from Eq. 11 are plotted in Fig. 4 (solid line) and match the experimental data quite well. In view of the similarity of Eqs. 3 and 11, the similarity in leakoff predictions is not surprising.

Model Differences

Although the predicted leakoff rate vs. time is approximately the same for both the new and conventional filtration models (see Fig. 4), the two are basically different and predict different behavior for several important properties. In the conventional model, the thickness of the filter cake is areally uniform (at least locally) and the entire fracture area continually experiences leakoff, the rate of which decreases because of a steady growth in the filter cake's thickness. In the new model, the filter cake is areally heterogeneous, leakoff is significant only on the fracture area that is contacted by wormholes, and the global leakoff rate decreases because of a continual loss of fracture area that is contacted by wormholes. As mentioned earlier, our observations of wormhole behavior during gel extrusion through fractures are consistent with the new model but inconsistent with the conventional filter-cake model.

In the conventional model (left side of Fig. 5), a single opening to flow exists that has a width equal to the fracture width minus twice the thickness of the filter cake at that point. The height of this opening is basically as high as the fracture. Thus, the flow opening is extremely high and narrow. In contrast, for a given distance along the fracture in the new model (right side of Fig. 5), multiple flow channels exist (corresponding to the wormholes), the width of each channel could be only slightly less than the original fracture width, and the height of each channel is small compared to the total fracture height (but generally large compared to the fracture width). As mentioned earlier, the conventional model incorrectly predicts that the width of the active flow path in the fracture decreases with increasing gel throughput (left side of Fig. 5) so that pressure gradients increase significantly with time. In contrast, in the new model, the width of the active flow path stays fairly constant with gel throughput and time (right side of Fig. 5), so the pressure gradient is independent of both, which is consistent with experimental observations (Fig. 1).

The two models predict significantly different flow and leakoff patterns as well as shear rates and stress levels within a fracture.¹⁸ These differences have important consequences for filter-cake erosion, propagation of gels and particulates along fractures, pressure transmission along fractures, fracture extension, and gel washout after placement. For a fixed pressure gradient, the new model predicts higher shear rates and shear stresses at the wall and much higher average fluid velocities than the conventional model.¹⁸ Consequently, greater filter-cake erosion is predicted in the new model than in the conventional model.

Of course, the pressure gradient along the fracture impacts gel propagation and washout in water-shutoff treatments and fracture extension in hydraulic fracturing and produced water reinjection (i.e., by affecting the pressure at the fracture tip).

Potential Use in Hydraulic Fracturing

Will the new model be a viable alternative to the conventional filter-cake model used in hydraulic fracturing? As mentioned previously, the new model quantitatively described leakoff for Cr(III)-acetate-HPAM gels quite well for a wide range of conditions. The new model was examined to determine whether it would work as well for a guar-borate gel commonly used during hydraulic fracturing. The gel contained 0.36% guar, 0.018% NaBO₂, 0.24% tallow soap, and 0.1% surfactant. This gel was aged for 1 day at 40°C and injected at 4,130 ft/D through a 6-in.-long, 0.04-in.-wide fracture. The experimental leakoff rates (see Fig. 7) were matched very well with the new model, even though it was developed to match the behavior of Cr(III)-acetate-HPAM gels. As with the Cr(III)-acetate-HPAM gel, the pressure gradient during extrusion of the guar-borate gel (through a second 6×1.5×0.04-in. fracture) was insensitive to the rate (i.e., pressure gradient rose by a factor of 2.3 as the injection flux increased from 206 to 33,000 ft/D).⁶

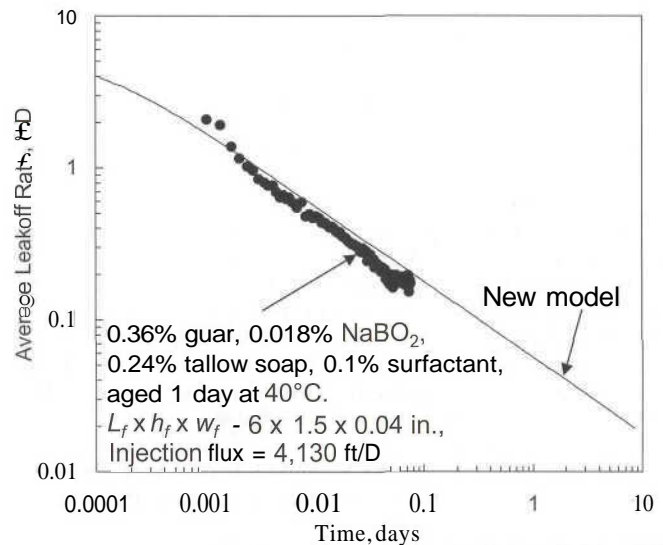


Fig. 7—Leakoff results for a guar-borate gel.

Of course, the time dependence of leakoff behavior in Fig. 7 does not prove that the new model is superior to the conventional one for guar-borate gels. Consequently, an extrusion experiment was performed with the guar-borate gel in a fracture in which $L_f \times h_f \times w_f = 12 \times 12 \times 0.04$ in. After performing an experiment similar to that associated with Fig. 3, the fracture was opened to view the wormhole pattern, as shown in Fig. 8. The presence of these wormhole patterns is consistent with our new model and inconsistent with the conventional filter-cake model. Also, during injection of the formed guar-borate gel, the pressure gradients did not rise monotonically as predicted by the conventional model (solid circles in Fig. 9). Thus, the guar-borate gel's behavior was more consistent with our new model than with the conventional one.

Effect of Temperature

Most of our experiments to date were performed at 41°C. Of course, many reservoirs and field applications exist at other (mostly higher) temperatures. Therefore, a need exists to determine gel extrusion and dehydration properties at other temperatures. With temperatures ranging from 20 to 80°C, extrusion experiments were performed with 650-md Berea sandstone cores of either 6- or 48-in. lengths. In each case, the fracture width was 0.04 in., and the fracture height was 1.5 in. Pressure taps along each 4-ft-long fracture divided the core into five sections of equal length, with a single set of pressure taps used for the 6-in.-long fractures. Effluent from the fracture and matrix were collected separately. We used our standard Cr(III)-acetate-HPAM gel [0.5%



Fig. 8—Wormhole pattern for a guar-borate gel.

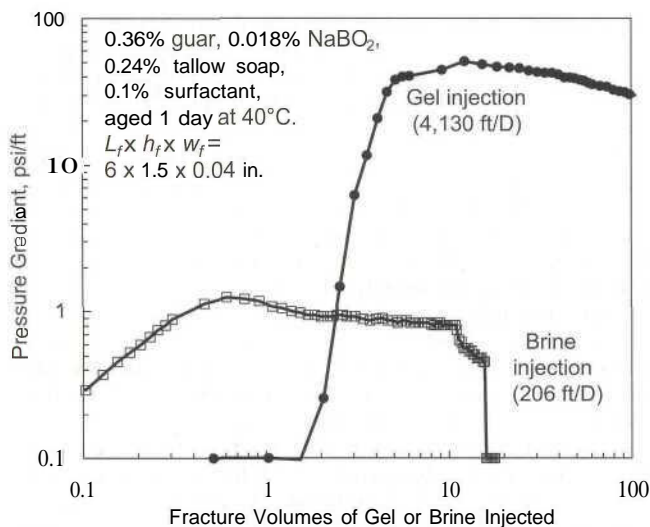


Fig. 9—Gel placement and washout for a guar-borate gel.

Ciba Alcoflood 93* HPAM, 0.0417% Cr(III) acetate] that was aged for 24 hours at 40°C before injection. The fractured core was equilibrated at the test temperature well before gel injection started. During injection of 226 in.³ (3700 cm³) of gel, the rate was fixed at 122 in.³/hr (2000 cm³/hr), translating to a flux in the fracture of 4,130 ft/D. Leakoff results from six sets of experiments are shown in Fig. 10. This figure shows that the leakoff behavior was not sensitive to temperature between 20 and 80°C, and pressure gradients during gel extrusion were also insensitive to temperature for these experiments.⁶ The elastic modulus (G') of this gel was also independent of temperature.¹⁹ In contrast, the viscosity of water decreased by a factor of approximately three as the temperature increased from 20 to 80°C.

For times shorter than 0.01 days (15 minutes), the leakoff data were very consistent with the predictions from our new leakoff model (solid curve in Fig. 10). For times longer than 0.01 days, the leakoff results exceeded the predictions associated with the new model, especially for the shorter cores. This deviation was suspected to be an artifact associated with the use of short fractures. In particular, some of the concentrated gel may be dislodged and produced from short fractures, thus permitting greater wormhole-fracture surface areas and higher leakoff rates for longer time periods. In longer fractures, the effect was less noticeable, although some deviation was noted at 40 and 60°C (see Fig. 10).

Effect of Gel Composition

Experiments were performed to investigate how gel extrusion and dehydration vary with gel composition. Most of our previous work used our "1X" gel containing 0.5% HPAM, 0.0417% Cr(III) acetate, 1% NaCl, and 0.1% CaCl₂. Recently, we tested a series of five compositions, including 1X, 1.5X, 2X, 2.5X, and 3X Cr(III)-acetate-HPAM gels. The multiplier refers to the HPAM and chromium concentrations relative to those in our standard 1X gel. In all cases, the HPAM/Cr(III)-acetate ratio was fixed at 12:1, and the gels were aged for 1 day at 40°C before injection at 4,130 ft/D (2000 cm³/hr) into 6-in.-long, 1.5-in.-diameter Berea sandstone cores that each contained a 0.04-in.-wide fracture. Because high pressure gradients were anticipated during extrusion of the concentrated gels, we used 6-in.-long cores cast in a metal alloy. Our 48-in.-long cores (cast in epoxy) would not withstand the required pressures.

Leakoff results from these five experiments are plotted in Fig. 11. Interestingly, the gels showed similar leakoff behavior. Predictions from the new model matched the leakoff results quite

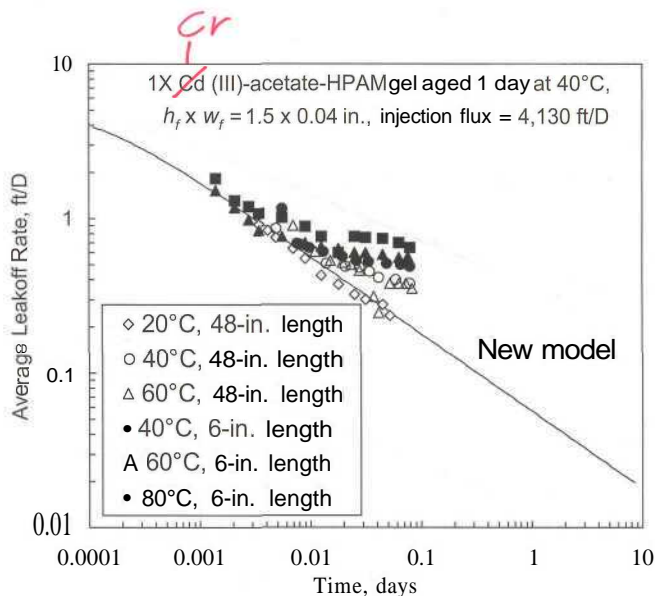


Fig. 10—Leakoff in fractures at different temperatures.

well for times less than 0.01 days. However, for longer times, the leakoff results exceeded the predictions. As mentioned previously, this deviation may be an artifact associated with the use of short fractures.

Pressure gradients during gel extrusion for the five experiments are plotted with solid circles in Fig. 12, which also plots the quantity, $2G'/w_f$ with open circles. The elastic modulus, G' , was measured over a range of gel compositions during separate experiments.¹⁹ Based on a force balance, the quantity $2G'/w_f$ should predict the pressure gradient required to extrude a gel through a fracture of a given width.¹⁹ Fig. 12 reveals that this force-balance approach typically underpredicts the pressure gradient by a factor of 87. Thus, more work is needed to relate rheological measurements to our extrusion results. However, the G' measurements paralleled the extrusion pressure gradients when plotted vs. gel composition. In Fig. 12, $2G'/w_f$ increased with $e^{2.27C}$ (in which C indicates the HPAM concentration in the gel). For the lower four gel compositions (1X to 2.5X), the pressure gradient for gel extrusion also varied with $e^{2.27C}$.

Gel Washout During Brine Injection

Cr(III)-Acetate-HPAM Gel. In many field applications, gel treatments were less effective than expected in reducing water production from fractured wells. Concern exists about the ability of gels

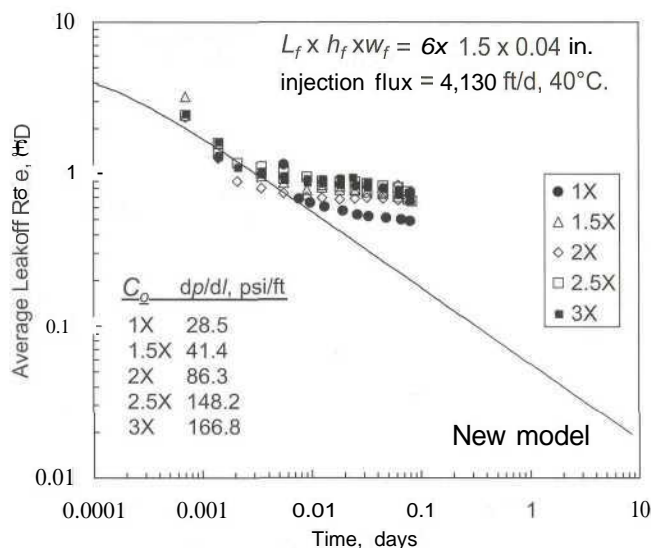


Fig. 11—Effect of gel composition during extrusion.

* Ciba Alcoflood 935 is trademarked to Ciba Specialty Chemicals, Tarrytown, New York (2002).

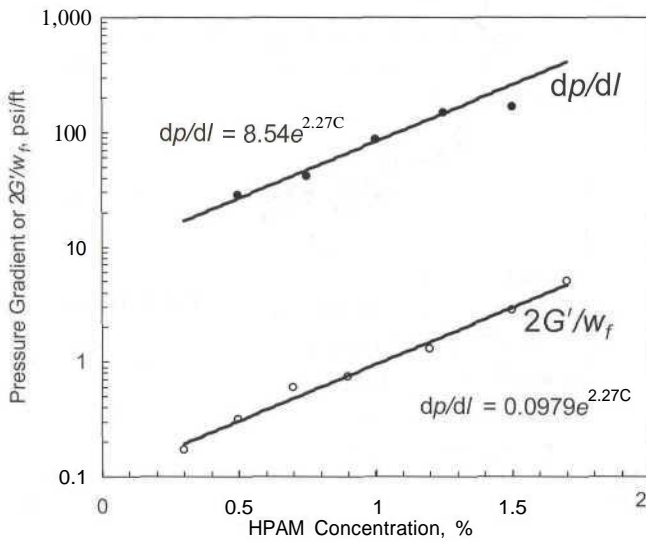


Fig. 12—Pressure gradient and elastic modulus vs. HPAM concentration.

to resist washout after placement. During brine flow after gel placement in a fracture, what pressure gradient is needed to remobilize the gel? To address this question, several experiments were performed in which brine was injected at various rates after gel placement. In all cases, the core material was 650-md Berea sandstone with a fracture placed lengthwise down the middle of each core. In each fractured core, 226 in.³ (3700 cm³) of 1-day-old Cr(III)-acetate-HPAM gel were injected at a rate of 122 in.³/hr (2000 cm³/hr). After gel placement, the core was shut in for 1 day. (These experiments were performed at 41°C.) Next, brine was injected at a low rate (e.g., 6.1 in.³/hr or 100 cm³/hr). A steady state was quickly established, and the pressure gradient was recorded. Then, the brine injection rate was doubled, and the measurements were repeated. This process was repeated in stages up to a final brine injection rate of 976 in.³/hr (16 000 cm³/hr), which was then decreased in stages.

Representative results were obtained with our standard 1X gel in a 0.04-in.-wide fracture. To a first approximation, the pressure gradient for gel failure was the same as that for gel extrusion through the fracture. The solid circles in Fig. 13 show that during gel injection (at 4,130 ft/D effective velocity in the fracture or 2000 cm³/hr), the pressure gradient rapidly rose to 17 psi/ft during the first 0.7 fracture volumes of gel injected. Thereafter, it was fairly stable during the course of injecting another 80 fracture

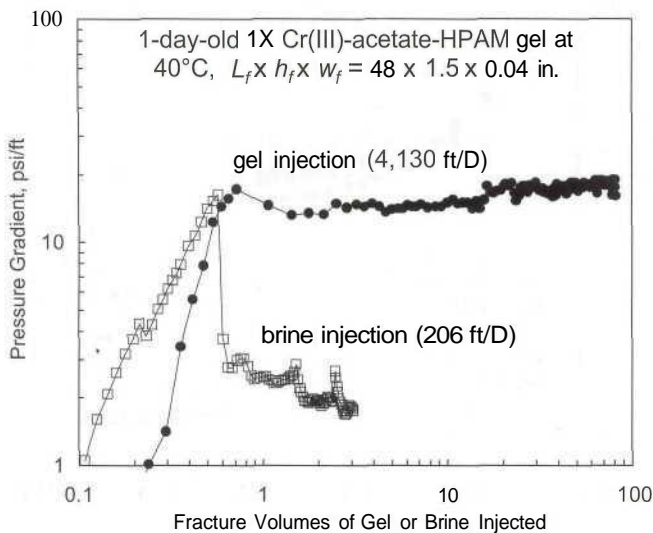


Fig. 13—Pressure gradients during gel vs. brine injection.

volumes of gel. When brine was subsequently injected (at 206 ft/D or 100 cm³/hr), the pressure gradient rapidly increased to 16 psi/ft within 0.6 fracture volumes. Thereafter, the pressure gradient dropped sharply, ending at 1.8 psi/ft after injecting three fracture volumes of brine.

Presumably, the gel in the wormholes provided the failure point during brine injection. This presumption was qualitatively consistent with the pressure gradients noted near the end of brine injection. Standard calculations for laminar flow of brine in tubes or slits²⁰ (coupled with the brine pressure gradients and flow rates) suggest that only approximately 10% of the gel washed out during brine injection. In contrast, if the entire gel mass had washed out, the brine pressure gradients should have been lowered by a factor of 7,000. Also, at the end of the experiment (i.e., after the rate studies described next), the fracture was opened, revealing that most of it was filled with concentrated gel.

The pressure gradients during brine injection at other rates are shown in Fig. 14. The open circles show the maximum pressure gradients (at a given rate) when the rates were increased in stages. Note that the maximum pressure gradient decreased for the first three rates in the sequence and then consistently rose for the higher rates. Presumably, brine displaced gel in the wormholes during injection at the lowest rate (see Fig. 13). For the next two rate increases, significant additional erosion of the gel occurred. For subsequent rate increases, gel erosion was less significant, although some probably occurred. During brine injection at 4,130 ft/D (2000 cm³/hr), the maximum pressure gradient was 26% less than the average during gel injection at the same rate (the solid square in Fig. 14).

The solid circles in Fig. 14 show the maximum pressure gradients when the rates were decreased in stages. At the final rate of 413 ft/D, the maximum pressure gradient was 1.7 psi/ft—much lower than the 9.0-psi/ft value noted at the same rate for the increasing rate part of the sequence.

The open diamonds in Fig. 14 show the average pressure gradients when rates were increased in stages, and the solid diamonds show the average pressure gradients when rates were decreased in stages. As expected, the pressure gradients for both curves increased monotonically with increased rate. Exposure to the increasing/decreasing rate cycle caused the average pressure gradient at 413 ft/D (200 cm³/hr) to decrease by 50% (from 2.4 to 1.2 psi/ft).

Of course, the objective of this kind of gel treatment is to dramatically reduce the flow capacity of the fracture so that fluid will flow through the porous rock instead. Fig. 15 plots the brine flow percentages through the fracture vs. through the matrix during brine injection after gel placement. At the first (and lowest) rate (206 ft/D or 100 cm³/hr), 100% of the flow occurred in the matrix, so the fracture was effectively plugged. Unfortunately, at higher

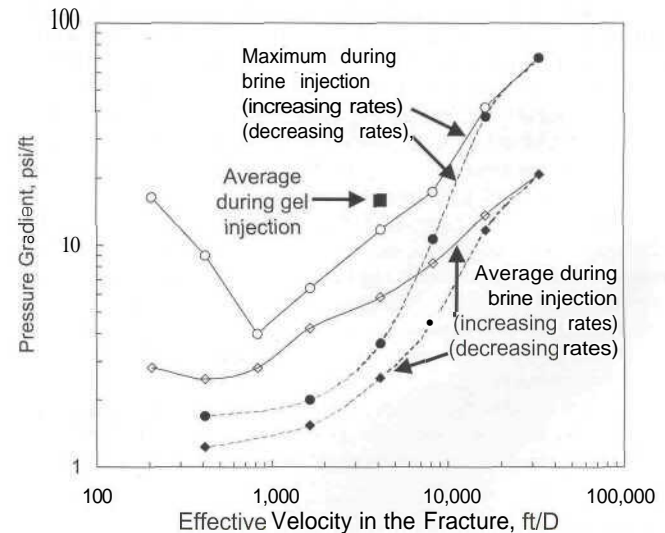


Fig. 14—Pressure gradients during brine flow at various rates.

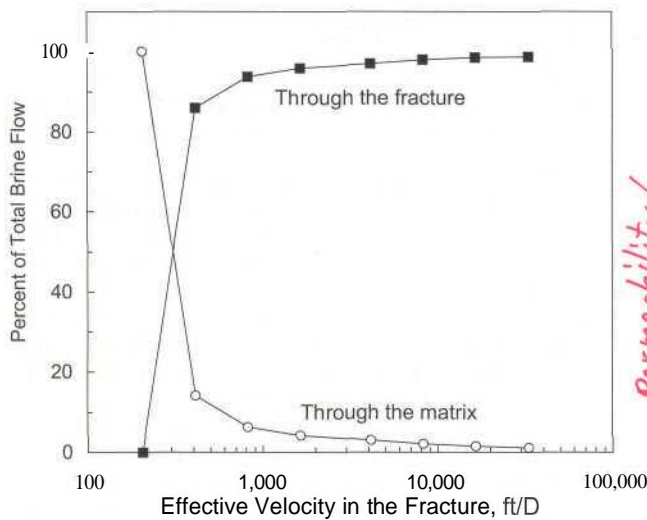


Fig. 15—Brine flow through fracture vs. matrix.

rates (i.e., after the gel plug experienced some washout), most flow occurred through the fracture. The gel substantially reduced (by a factor greater than 500) the flow capacity of the fracture throughout various brine injection stages even at the highest flow rate. However, this fact may seem a minor consolation because the fracture still dominated the flow capacity of the system.

Figs. 13 through 15 indicate that the greatest damage to the gel occurred during the first exposure to a pressure gradient similar to that during gel injection. Exposure to larger pressure gradients certainly caused additional damage to the gel. However, the incremental damage was less severe than that after the first large pressure pulse (Fig. 13). This behavior is consistent with gel of the original composition being washed out of wormholes. Presumably, larger pressure gradients were required to erode the more concentrated gel.

Guar-Borate Gel. A similar washout experiment was performed after placing the guar-borate gel in the previously described core (Fig. 9). During gel injection, the pressure gradient rose to a value of 51 psi/ft (at 12 fracture volumes), followed by a gradual decline to 30 psi/ft after 100 fracture volumes of gel. During brine injection, the peak pressure gradient of 1.2 psi/ft was reached at 0.8 fracture volumes, and a dramatic decrease occurred at 16 fracture volumes. Thus, the guar-borate gel washed out of the fracture much easier than the 1X Cr(III)-acetate-HPAM gel. This behavior may be desirable for hydraulic fracturing because "fracture cleanup" is important in these applications. In contrast, the greater resistance to washout exhibited by the Cr(III)-acetate-HPAM gel is more desirable for water-shutoff applications. Nonetheless, increased resistance to washout is needed for these gels.

Washout With Wider Fractures and More Concentrated Gels

Experiments were performed to examine how gel washout was affected by fracture width and gel concentration. The results from many of these experiments are shown in Fig. 16. The y-axis plots the final core permeability relative to that of an unfractured core. A y-value of unity or less means that the fracture was basically "healed." As the y-value increased to greater than one, the fracture became more open or conductive, indicating a greater degree of gel washout. The x-axis plots the steady-state pressure gradient during brine injection relative to that during gel injection. As expected, the pressure gradient during gel injection increased with decreased fracture width and increased polymer concentration.

Three experiments were performed with our standard 1X gel (the open symbols in Fig. 16). Two experiments were performed with a 2X gel (solid symbols in Fig. 16) that contained twice the HPAM and Cr(III)-acetate concentrations of the 1X gel. For both the 1X and 2X gels in 0.04-in.-wide fractures, the y-value (core

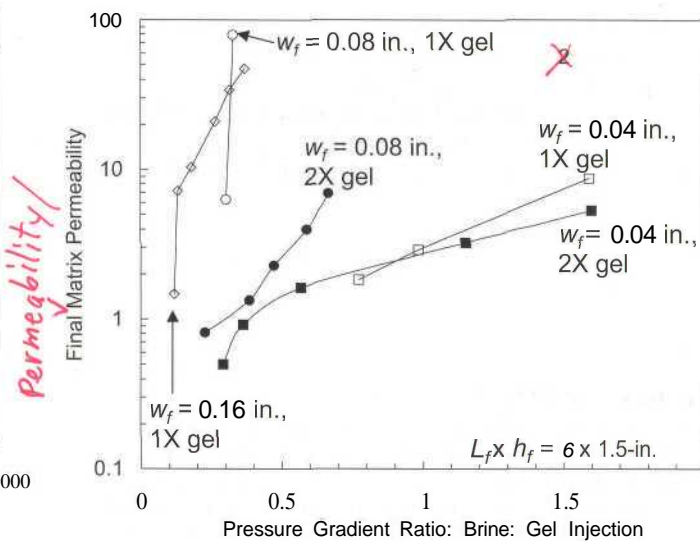


Fig. 16—Gel washout during brine injection after gel placement.

permeability ratio) began at less than unity and increased moderately for pressure-gradient ratios between 0.5 and 1.5. This result indicates that in a 0.04-in.-wide fracture, gel mobilization during brine injection occurred at pressure gradients similar to those during gel injection. In wider fractures (0.08 and 0.16 in.), the 1X gel experienced mobilization (steep slopes in Fig. 16) at pressure-gradient ratios between 0.1 and 0.3. For the 2X gel in a 0.08-in.-wide fracture, intermediate mobilization behavior was noted.

Conclusions

1. A new model was developed to describe water leakoff from formed Cr(III)-acetate-HPAM gels during extrusion through fractures. This model is fundamentally different from the conventional filter-cake model that was used during hydraulic fracturing. Even so, the model accurately predicted leakoff during extrusion of a guar-borate gel and may be of interest in hydraulic fracturing.
2. Contrary to the conventional model, the new model correctly predicted the occurrence of wormholes and stable pressure gradients during gel extrusion through fractures.
3. During extrusion of a formed Cr(III)-acetate-HPAM gel, pressure gradients and gel dehydration were similar from 20 to 80°C.
4. Similar gel dehydration behavior was observed over a three-fold range of concentration for Cr(III)-acetate-HPAM gels. During extrusion, measurements of pressure gradient vs. HPAM concentration paralleled those of elastic modulus vs. HPAM concentration.
5. In 0.04-in.-wide fractures, gel mobilization during brine injection occurred at pressure gradients similar to those during gel injection. In wider fractures (0.08- and 0.16-in.), Cr(III)-acetate-HPAM gels experienced mobilization at lower-than-expected pressure gradients.

Nomenclature

- A_c = fraction of area contacted by concentrated gel
- A_m = fraction of area contacted by mobile gel
- C = gel or polymer concentration, g/m^3 or %
- C_o = original concentration of gel, g/m^3
- G' = elastic modulus, psi [kPa]
- h_f = fracture height, ft [m]
- k = permeability, darcies [μm^2]
- k_f = fracture permeability, darcies [μm^2]
- k_{gel} = inherent permeability of gel to water, darcies [μm^2]
- l = length, ft [m]
- L = distance across a filter cake, ft [m]
- L_f = fracture length, ft [m]

p = pressure, psi, [kPa]
 t = time, days
 t_{exp} = time since first exposure, days
 u_c = water leakoff rate from concentrated gel, ft/D [m/D]
 u_l = water leakoff rate, ft/D [m/D]
 u_m = water leakoff rate from mobile gel, ft/D [m/D]
 w = width, ft [m]
 w_f = fracture width, ft [m]
 a = suspension-filter-cake concentration factor
 Δp = pressure difference, psi [kPa]
 μ = viscosity, cp [Pa·s]
 μ_o = viscosity of a Newtonian fluid, cp [Pa·s]

Acknowledgments

Financial support for this work from the Natl. Petroleum Technology Office of the U.S. Dept. of Energy, BP, Chevron, China Natl. Petroleum Corp., Chinese Petroleum Corp., Intevep/PDVSA, Marathon, Phillips, Shell, and Texaco is gratefully acknowledged. I thank Richard Schrader for performing the experiments and Norman Warpinski of Sandia for reviewing the new filter-cake idea in advance. I appreciated useful discussions with Jenn-Tai Liang (INEEL), Jim Morgan (BP), Robert Sydansk and Robert Lane (Northstar), and Amaury Marin (Intevep/PDVSA). Thanks also to Prentice Creel (Halliburton) for providing the components for the guar-borate gel.

References

1. Seright, R.S.: "Polymer Gel Dehydration During Extrusion Through Fractures," *SPEPF* (May 1999) 110.
2. Seright, R.S.: "Mechanism for Gel Propagation Through Fractures," paper SPE 55628 presented at the 1999 SPE Rocky Mountain Regional Meeting, Gillette, Wyoming, 15-19 May.
3. Seright, R.S.: "Use of Preformed Gels for Conformance Control in Fractured Systems," *SPEPF* (February 1997) 59.
4. Seright, R.S.: "Gel Propagation Through Fractures," *SPEPF* (November 2001) 225.
5. Seright, R.S.: "Using Chemicals to Optimize Conformance Control in Fractured Reservoirs," Annual Technical Progress Report (U.S. DOE Report DOE/BC/15110-4), U.S. DOE Contract DE-AC26-98BC15110 (2000) 3.
6. Seright, R.S.: "Using Chemicals to Optimize Conformance Control in Fractured Reservoirs," Annual Technical Progress Report (U.S. DOE Report DOE/BC/15110-6), U.S. DOE Contract DE-AC26-98BC15110 (2001) 40.
7. Howard, G.C. and Fast, C.R.: *Hydraulic Fracturing*, Monograph Series, SPE, Richardson, Texas (1970) 2, 32.
8. Howard, G.C. and Fast, C.R.: Optimum Fluid Characteristics for Fracture Extension," *Drilling and Production Practices*, API (1957) 261.
9. Penny, G.S. and Conway, M.W.: "Fluid Leakoff," *Recent Advances in Hydraulic Fracturing*, J.L. Gidley *et al.* (eds.), Monograph Series, SPE, Richardson, Texas (1989) 12, 147.
10. Mack, M.G. and Warpinski, N.R.: "Mechanics of Hydraulic Fracturing," *Reservoir Stimulation*, third edition, John Wiley, New York City (2000) Chapter 6.

11. Constien, V.G. *et al.*: "Performance of Fracturing Materials," *Reservoir Stimulation*, third edition, John Wiley, New York City (2000) Chapter 8.
12. His, C.D. *et al.*: "Formation Injectivity Damage Due to Produced Water Reinjection," paper SPE 27395 presented at the 1994 SPE International Symposium on Formation Damage Control, Lafayette, Louisiana, 7-10 February.
13. Martins, J.P. *et al.*: "Long-Term Performance of Injection Wells at Prudhoe Bay: The Observed Effects of Thermal Fracturing and Produced Water Re-Injection," paper SPE 28936 presented at the 1994 SPE Annual Technical Conference and Exhibition, New Orleans, 25-28 September.
14. Bedrikovetsky, P. *et al.*: "Well Impairment During Sea/Produced Water Flooding: Treatment of Laboratory Data," paper SPE 69546 presented at the 2001 SPE Latin American and Caribbean Petroleum Engineering Conference, Buenos Aires, 25-28 March.
15. Ganguly, S., Wilhite, G.P., and McCool, C.S.: "The Effect of Fluid Leakoff on Gel Placement and Gel Stability in Fractures," *SPEJ* (September 2002) 309.
16. Seright, R.S.: "Conformance Improvement Using Gels," Annual Technical Progress Report (U.S. DOE Report DOE/BC/15316-2), U.S. DOE Contract DE-AC26-01BC15316 (2002) 2.
17. Seright, R.S.: "Using Chemicals to Optimize Conformance Control in Fractured Reservoirs," Annual Technical Progress Report (U.S. DOE Report DOE/BC/15110-2), U.S. DOE Contract DE-AC26-98BC15110 (1999) 3.
18. Seright, R.S.: "An Alternative View of Filter Cake Formation in Fractures," paper SPE 75158 presented at the 2002 SPE/DOE Improved Oil Recovery Symposium, Tulsa, 13-17 April.
19. Liu, J. and Seright, R.S.: "Rheology of Gels Used for Conformance Control in Fractures," *SPEJ* (June 2001) 120.
20. Bird, R.B., Stewart, W.E., and Lightfoot, E.N.: *Transport Phenomena*, John Wiley & Sons, New York (1960) 11, 42.

SI Metric Conversion Factors

cp × 1.0*	E-03 = Pa·s
ft × 3.048*	E-01 = m
ft ² × 9.290 304*	E-02 = m ²
ft ³ × 2.831 685	E-02 = m ³
°F (°F-32)/1.8	= °C
in. × 2.54*	E+00 = cm
in. ² × 6.451 6*	E+00 = cm ²
in. ³ × 1.638 706	E+01 = cm ³
md × 9.869 233	E-04 = μm ²
psi × 6.894 757	E+00 = kPa

*Conversion is exact.

Randy Seright is a senior engineer at the New Mexico Petroleum Recovery Research Center at New Mexico Tech in Socorro. e-mail: randy@prcc.nmt.edu. Seright holds a PhD degree in chemical engineering from the U. of Wisconsin at Madison.